JOURNAL OF VIROLOGY, Apr. 2006, p. 3273–3284 Vol. 80, No. 7
0022-538X/06/$08.00+0 doi:10.1128/JVI.80.7.3273–3284.2006

Astrocytes Survive Chronic Infection and Cytopathic Effects of the *ts*1 Mutant of the Retrovirus Moloney Murine Leukemia Virus by Upregulation of Antioxidant Defenses

Wenan Qiang,*† Xianghong Kuang,‡ Jinrong Liu,§ Na Liu, Virginia L. Scofield, Amy J. Reid, Yuhong Jiang, Gheorghe Stoica,¶ William S. Lynn, and Paul K. Y. Wong*

Department of Carcinogenesis, The University of Texas M. D. Anderson Cancer Center, Science Park-Research Division, P.O. Box 389, Smithville, Texas 78957

Received 28 July 2005/Accepted 10 January 2006

The *ts*1 mutant of Moloney murine leukemia virus (MoMuLV) induces a neurodegenerative disease in mice, in which glial cells are infected by the retrovirus but neurons are not. *ts*1 infection of primary astrocytes, or of the immortalized astrocytic cell line C1, results in accumulation of the *ts*1 gPr80^{env} envelope protein in the endoplasmic reticulum (ER), with ER and oxidative stress. Notably, only about half of the infected astrocytes die in these cultures, while the other half survive, continue to proliferate, and continue to produce virus. To determine how these astrocytes survive *ts*1 infection in culture, we established a chronically infected subline of the living cells remaining after the death of all acutely infected cells in an infected C1 cell culture (C1-*ts*1-S). We report here that C1-*ts*1-S cells proliferate more slowly, produce less virus, show reduced H_2O_2 levels, increase their uptake of cystine, and maintain higher levels of intracellular GSH and cysteine compared to acutely infected or uninfected C1 cells. C1-*ts*1-S cells also upregulate their thiol antioxidant defenses by activation of the transcription factor NF-E2-related factor 2 (Nrf2) and its target genes. Interestingly, despite maintenance of higher levels of intracellular reduced thiols, C1-*ts*1-S cells are more sensitive to cystine deprivation than uninfected C1 cells. We conclude that some *ts*1-infected astrocytes survive and adapt to virus-induced oxidative stress by successfully mobilizing their thiol redox defenses.

Infection of FVB/N mice at birth with the *ts*1 retrovirus, a mutant of Moloney murine leukemia virus (MoMuLV), induces a progressive neuroimmunodegenerative disease that resembles human immunodeficiency virus (HIV) infection/AIDS in several important ways (10, 43, 44). The characteristic features of *ts*1-induced disease are T-cell depletion, from the thymus and peripheral lymphoid tissues, and neuronal loss and astrogliosis in the central nervous system (CNS), with the latter leading to hind-limb paralysis and death by 30 to 40 days postinfection (p.i.) (42, 44, 46). T cells are the primary peripheral targets for both HIV and *ts*1 MoMuLV. Macrophages are also targets for both viruses. As in HIV infection, *ts*1-infected macrophages survive productive infection, although infected T cells die (31, 36, 40).

In the CNS, both HIV and *ts*1 infect microglia and astrocytes, but not neurons (10, 43). These findings suggest that the profound neuronal loss induced by these retroviruses is not directly due to infection of neurons, but rather to impairment of neuronal support by astrocytes or to secretion of neurotoxic factors by infected or activated astrocytes and microglia. Notably, in the spongiform lesions seen in the *ts*1-infected CNS, some astrocytes die, but others survive and are alive 30 days p.i., when infected mice become paralyzed (4, 37, 38).

In our hands, primary astrocytes and continuous astrocyte cultures were infected with *ts*1 at a multiplicity of infection of 5 to 10, to ensure that all cells were infected when the inoculum was added. Under these conditions, cytopathic effects and cell death were evident in the cultures by 3 to 4 days p.i., although as noted above, only about half of the cells in these cultures died. The surviving cells continued to proliferate slowly and maintained low levels of progeny virus production (33, 37) if fresh medium was provided and the cells were passaged. From these observations, we hypothesized that some *ts*1-infected astrocytes mounted defenses that allowed them to survive while replicating virus, although the initial differences between these cells and those that died were unclear and the mechanisms for the adaptations were unknown. We therefore set out to identify adaptations deployed in these "survivor" cells that enabled them to survive and maintain virus infection.

Due to the limited life span of primary neonatal astrocytes in culture, we were unable to use these cells to establish the long-term cultures of infected "survivor" cells necessary to study the survival mechanisms developed by the cells after *ts*1 infection. To circumvent this drawback, we used a previously developed immortalized clonal astrocyte line called C1 (18). Cultured C1 cells resemble primary astrocytes in many ways,

* Corresponding author. Mailing address for P. K. Y. Wong: Department of Carcinogenesis, The University of Texas M. D. Anderson Cancer Center, Science Park-Research Division, P.O. Box 389, Smithville, TX 78957. Phone: (512) 237-9456. Fax: (512) 237-2444. E-mail: pkwong@mdanderson.org. Mailing address for W. Qiang: 303 E. Chicago Ave., Searle 7-457, Chicago, IL 60611-3008. Phone: (312) 503-3221. Fax: (312) 503-3202. E-mail: w-qiang@northwestern.edu.

† Present address: Department of Cell and Molecular Biology, Northwestern University Feinberg School of Medicine, Chicago, IL 60611.

‡ Present address: Department of Pharmacology, School of Basic Medical Sciences and Forensic Medicine, Sichuan University, Chengdu, People's Republic of China.

§ Present address: Drug Metabolism Department, Abbott Laboratories, Abbott Park, IL 60064.

¶ Present address: Department of Pathobiology, Texas A&M University College of Veterinary Medicine, College Station, TX 77843.

including typical astrocytic morphology, expression of the astrocyte markers GFAP and vimentin, contact inhibition at confluence, and ready infection by *ts*1 (18, 33). In addition, C1 astrocytic cells respond to *ts*1 infection as do primary astrocytes, including the appearance of a survivor cell population (18, 19), accumulation of $gPr80^{env}$ in the endoplasmic reticulum (ER), the onset of ER stress (19), intracellular accumulation of reactive oxygen species (ROS), activation of the redox-sensitive transcription factor NF-E2-related factor 2 (Nrf2), and upregulation of Nrf2-coupled antioxidant response element (ARE)-mediated defenses involving cystine uptake and glutathione (GSH) synthesis (27).

We surmise that C1 astrocytes that succumb to *ts*1 infection die by oxidative-stress-induced apoptosis. This implies that those cells that survive remain alive because of their successful mobilization of Nrf2-mediated thiol antioxidative defenses previously described from our work with infected C1 cultures (27). To determine whether these factors contribute to cell survival in the cells that do not die, we established a subline of the chronically infected "survivor" C1 cells (C1-*ts*1-S). We then compared these cells to uninfected C1 cells and to acutely infected C1 cells (C1-*ts*1), where appropriate, for the presence of physiological markers correlated with activation of Nrf2-mediated antioxidant defense pathways in astrocytes. We were interested in characteristics of C1-*ts*1-S cells that distinguish them both from uninfected C1 cells and from acutely infected C1-*ts*1 cells; thus, this work required comparisons of C1-*ts*1-S cells to uninfected C1 cells for some parameters and to C1-*ts*1 cells for others.

We report here that C1-*ts*1-S cells proliferate more slowly than uninfected C1 cells, increase their levels of ER chaperone proteins in relation to those in uninfected C1 cells, and increase their levels of the prosurvival factor Bcl-2 relative to levels in uninfected C1 cells. C1-*ts*1-S cells also contain significantly elevated amounts of activated Nrf2 and its downstream target gene products compared to uninfected C1 cells. Finally, C1-*ts*1-S cells exhibit increased cystine uptake and GSH synthesis relative to uninfected C1 cells and contain reduced levels of intracellular ROS compared to C1-*ts*1 cells. The data imply that C1-*ts*1-S cells mobilize and maintain enhanced intracellular thiol redox defenses relative to uninfected C1 cells. Together, these adjustments allow C1-*ts*1-S cells to maintain intracellular ROS levels after infection that are lower than those in C1-*ts*1 cells, resulting in their surviving *ts*1-induced oxidative stress. These results show that some murine astrocytes survive *ts*1 infection via activation of their Nrf2-mediated thiol antioxidant defenses and that such cells continue to produce infectious virus for an indefinite amount of time.

MATERIALS AND METHODS

Virus titer and *ts*1 infection. *ts*1, a spontaneous temperature-sensitive mutant of MoMuLV-TB, was propagated in TB cells, a thymus-bone marrow cell line. Virus titers were determined by a modified direct focus-forming assay in the 15F cell line, a murine sarcoma virus-positive, leukemia-virus-negative cell line, as described previously (48).

Mice and infection. FVB/N mice were obtained from Taconic Farms (Germantown, NY). Breeding pairs were housed in sterilized microisolator cages and supplied with autoclaved food and water ad libitum. The microisolators were kept in an environmentally controlled isolation room. For *ts*1 infection, 1-day-old mice were inoculated intraperitoneally with 0.1 ml of vehicle (mock infection) or with 0.1 ml of a *ts*1 suspension containing 1×10^6 to 5×10^6 infectious units/ml. Mice from all groups were observed daily for clinical signs of disease, and some individuals from all groups were sacrificed at 21 or 30 days p.i. The brainstems and spinal cords were removed, snap-frozen in liquid nitrogen, and kept at −80°C until they were used for cysteine and GSH assays. These infection, animal maintenance, and euthanasia protocols were approved by The University of Texas M. D. Anderson Cancer Center Institutional Animal Care and Use Committee.

Establishment of the *ts*1-resistant C1-*ts*1-S cell line. Immortalized murine C1 astrocytes were established as previously described (18). Briefly, primary astrocytes from FVB/N mice were transfected with sequences encoding a temperature-sensitive form of the simian virus 40 T antigen (tsA58). The advantage of using this conditional-mutant T antigen for transformation of the C1 cells is that the mitogenic drive of the T antigen can be suppressed simply by shifting the incubation temperature of the cells from permissive (33 to 34°C) to restrictive (37 to 38°C) temperature. At this temperature, which is the temperature at which our cells are incubated, the C1 cells differentiate and behave like primary astrocytes and, like primary astrocytes, are readily infected with *ts*1.

To establish the "survivor" cell line from *ts*1-infected C1 cells, C1 astrocytes were seeded at 1×10^6 cells/well in 100-mm plastic tissue culture dishes and incubated overnight in Dulbecco's modified Eagle's medium (DMEM) containing 1% fetal bovine serum (FBS) and 3 μg/ml Polybrene to enhance viral adsorption. The next day, the cells were infected with *ts*1 for 40 min at a multiplicity of infection of 10 in a 37°C CO_2 incubator. The cells were then washed and refed with fresh DMEM containing 10% FBS. As noted above, approximately 50% of the cells in these cultures typically died by 3 to 5 days p.i. At that time, cultures containing dead and surviving cells were fed fresh DMEM every 3 or 4 days until the surviving cells were confluent, and then the cells were passed into new culture dishes. This was continued for 2 months, producing a stable subline of immortalized C1 astrocytes that were chronically infected with *ts*1 (C1-*ts*1-S).

Cell viability. To compare the relative sensitivities of C1-*ts*1-S and uninfected C1 cells to cystine-limited conditions, both cell types were plated at 4×10^5 cells per 60-mm plate in DMEM containing different concentrations of cystine. The media for all cultures contained 10% FBS but were supplemented with stepped concentrations of cystine (0, 10, 100, 200, 500, or 1,000 μM cystine [Invitrogen, Carlsbad, CA]). Untreated, cystine-starved, and cystine-supplemented cells from both cultures were then tested either for viability, by trypan blue exclusion at 24, 48, or 72 h p.i., or for their GSH content (see below). For cell counting, cells were trypsinized, suspended, stained with trypan blue for 5 min, and then counted with a hemocytometer.

Cell cycle analysis. C1 or C1-*ts*1-S cells (1×10^6) were cultured for 16 h in 100-mm plastic petri dishes in DMEM containing 1% FBS, after which fresh DMEM containing 10% FBS was added. At 0, 24, 48, and 72 h of incubation, the cells were trypsinized, fixed in 70% ethanol, and stained with propidium iodide containing RNase. The DNA content was analyzed by flow cytometry on a Coulter Epics Elite flow cytometer. Cell cycle analysis was performed with Multicycle software (Phoenix Flow Systems, San Diego, CA).

Intracellular GSH content. Levels of intracellular GSH were determined as previously described (27), using a GSH assay kit (Calbiochem, San Diego, CA). In brief, C1 or C1-*ts*1-S cells were plated at a density of 2×10^6 cells per 100-mm dish. Some of the C1 cell cultures were infected with *ts*1 virus as described above. For comparisons of GSH levels under cystine-deficient conditions, cells were cultured for 24, 48, or 72 h in cystine-deficient DMEM with 10% FBS, to which increasing supplemental concentrations of cystine (0, 10, 100, 200, 500, or 1,000 μM cystine) were added. At each of the three time points, C1 or C1-*ts*1-S cell cultures were washed twice with phosphate-buffered saline (PBS) and then collected by centrifugation. The resulting pellets were homogenized in ice-cold 5% metaphosphoric acid solution and then recentrifuged to obtain supernatants for the measurement of absorbance at 400 nm.

Brainstem and spinal cord tissues were harvested from *ts*1-infected and uninfected mice at 30 days p.i., and their GSH contents were determined as described above. After homogenization in ice-cold 5% metaphosphoric acid solution, the tissues were centrifuged and supernatants were harvested for measurement of their absorbance at 400 nm. The protein contents of homogenized cells and tissues were determined for each sample with a bicinchoninic acid (BCA) protein assay kit (Pierce, Rockford, IL). The GSH content is expressed as the number of nanomoles of GSH per milligram of protein.

Total extra- and intracellular cystine/cysteine content. Total extra- and intracellular cystine/cysteine was measured by fluorometric high-performance liquid chromatography (HPLC), as described previously (27, 35, 45). C1 or C1-*ts*1-S cells were plated at a density of 2×10^6 cells per 100-mm dish. At 24, 48, or 72 h of incubation, the culture medium was collected, and the cell monolayers were washed three times with PBS, harvested, and pelleted; 1.5 M $HClO_4$ was then

added to the supernatants, while the cells in the pellet were resuspended in 0.5 M $HClO_4$. Both the supernatants and pellet suspensions were then neutralized with 2 M $KHCO_3$ and centrifuged at 14,000 rpm for 20 min. The supernatants from this centrifugation step were collected and frozen at −80°C for later measurement of the total extra- and intracellular cystine/cysteine content, while the pellets were retained for protein content measurements. For measurement of total extra- and intracellular cystine/cysteine, the frozen samples were thawed, followed by reduction of cystine to cysteine in the presence of 2-mercaptoethanol, and then by conversion of total cysteine to *S*-carboxymethylcysteine in the presence of iodoacetate. *S*-carboxymethylcysteine reacts with *o*-phthaldialdehyde to form a fluorescent derivative that can be measured by fluorometric HPLC. Cysteine in the samples was quantified with the aid of cysteine standards (Sigma, St. Louis, MO). The protein content was then determined with a BCA protein assay kit. Total intracellular cysteine levels from these determinations were expressed as nmol cysteine per mg of protein, and total extracellular cystine/cysteine content was expressed as nmol of cysteine per ml of culture medium.

Brainstem and spinal cord tissues were harvested from *ts*1-infected and uninfected mice at 30 days p.i. The tissues were homogenized in 0.5 M $HClO_4$, neutralized with 2 M $KHCO_3$ and then centrifuged at 14,000 rpm for 20 min. Measurements of total cystine/cysteine in the tissue samples was done using the same procedures described above. The cystine/cysteine content was expressed as nmol cysteine per mg of protein.

Intracellular ROS (H_2O_2) assay. Intracellular ROS (H_2O_2) levels were measured using the dye 5 (and 6)-chloromethyl-2,7-dichlorodihydrofluorescein diacetate (CM-H2DCFDA) (Molecular Probes, Eugene, OR), as described previously (17, 27). In brief, C1 or C1-*ts*1-S cells were plated as described above. The C1 cells were then either mock infected or infected with the *ts*1 virus. Some of the cell cultures in each experiment were treated with 1 mM buthionine sulfoximine (BSO) (Sigma), an inhibitor of GSH synthesis (24), for the last 24 h of incubation. These BSO-treated cells served as positive control cultures for induced oxidative stress (uninfected C1 cells) or to test for amplified oxidative stress (C1-*ts*1-S cells).

After 24, 48, or 72 h of incubation, all cells were loaded with 10 μM of CM-H_2DCFDA dye in the culture medium for a final 30 min at 37°C. The dye-loaded cells were then harvested, and their forward and side scatter DCFDA fluorescence profiles were determined by flow cytometry using a Coulter Epics Elite software program, version 4.02.

Western blotting analysis. Total cellular proteins were prepared with modified radioimmunoprecipitation assay buffer as described previously (27). Separate nuclear and cytoplasmic fractions were prepared with the NE-PER nuclear and cytoplasmic extraction kit (Pierce), and cross-contamination between the fractions was verified as being less than 5% by Western blotting with cytosol- and nuclear-protein-specific antibodies. Protein concentrations were determined with the *DC* protein assay reagent (Bio-Rad Laboratories, Hercules, CA). The cell lysates (20 to 50 μg of total protein per sample) were separated on sodium dodecyl sulfate-polyacrylamide gels with 10 or 12% polyacrylamide. After electrophoresis, the proteins were transferred to polyvinylidene difluoride membranes (Millipore Corp., Bedford, MA). The blotted membranes were blocked for 1 h in Tris-buffered saline with 5% nonfat milk at room temperature and subsequently incubated with primary antibodies against the proteins of interest.

Rabbit anti-catalase antibody was purchased from Rockland, Inc. (Gilbertsville, PA); rabbit anti-GPx was from Chemicon International (Temecula, CA); rabbit anti-γ-GCLC was a gift from T. J. Kavanagh of the University of Washington; rabbit anti-xCT and rabbit anti-γ-GCLM polyclonal antibodies were prepared in our laboratory, as described previously (27), and affinity purified (Bethyl Laboratories, TX); mouse monoclonal anti-Bcl-2, rabbit anti-Nrf2, rabbit anti-GRP78, and rabbit anti-GRP94 antibodies were from Santa Cruz Biotechnology, Inc. (Santa Cruz, CA); rabbit anti-calreticulin (CalR) was from Sigma, and goat anti-gp70 was from ViroMed Biosafety Laboratories (Camden, NJ).

After incubation with the primary antibody, the polyvinylidene difluoride membranes were washed and incubated with horseradish peroxidase-conjugated secondary antibodies (anti-rabbit [Amersham Biosciences, Piscataway, NJ], anti-goat [Sigma], and anti-mouse [Bio-Rad Laboratories]). Immune complexes were detected on the membranes with a chemiluminescent reagent (NEN Life Science Products, Boston, MA). An anti-β-actin monoclonal antibody (Sigma) was used as a control for protein loading. Net intensities of protein bands of interest were acquired through densitometric analysis of autoradiographs using a Kodak Digital Science Image Station 440 CF and 1D Image Analysis software (Kodak, Rochester, NY). Band intensities were then normalized to β-actin intensities and compared for differences between experimental and control conditions. All Western blotting results were replicated in three to five independent experiments.

Cystine uptake. For measurement of cystine uptake by C1 or C1-*ts*1-S cells, the cells were plated at a density of 2×10^6 cells per 35-mm dish and incubated for 24 h. The monolayers were then washed and incubated in bicarbonate buffer medium (122 mM NaCl, 3 mM KCl, 25 mM $NaHCO_3$, 1.3 mM $CaCl_2$, 1.2 mM KH_2PO_4, 0.4 mM $MgSO_4$, and 10 mM glucose) for 20 min at 37°C in 5% CO_2, followed by addition of 0.5 μCi/ml of L-[^{35}S]cystine (Amersham Pharmaceuticals, Piscataway, NJ) to each culture in 100 μM of unlabeled L-cystine and incubation of the cultures for an additional 3 min. The uptake of [^{35}S]cystine (1) was terminated by washing the cells three times with ice-cold bicarbonate buffer. The cells were then solubilized in 0.5 ml of 0.5 N NaOH for 30 min, and 300 μl of each lysate was added to 5 ml scintillation solution for measurement of radioactivity in a Beckman LS6500 liquid scintillation counter (Beckman Coulter, Fullerton, CA). Another 50 μl of the lysate was used for protein content determination, using a BCA protein assay kit. Cystine uptake rates from these determinations were expressed as nmol cystine taken up by the cells/min/mg of protein.

γ-GT activity. γ-Glutamyltranspeptidase (γ-GT) enzymatic activity was determined in whole-cell lysates using a commercially available γ-glutamyl transferase kit (Sigma). For this assay, 5×10^6 C1 or C1-*ts*1-S cells were plated in 100-mm dishes. Some of the cultures were treated with 200 μM of acivicin, a specific inhibitor of γ-GT (9), for the last 4 h of their 24-hour incubation. After incubation, the cells were washed three times with PBS, harvested, and then pelleted. The cell pellets were lysed and incubated on ice for 10 min and then centrifuged at 14,000 rpm for 4 min; 50 μl of the resulting lysate from each pellet was then added to 0.5 ml of prewarmed γ-GT substrate. After 1 h of incubation at 37°C, 1 ml of 10% acetic acid was added to each tube, followed by 0.5 ml of sodium nitrite solution. After being mixed, each tube was incubated at room temperature for 3 min, at which time 0.5 ml of ammonium sulfamate solution was added, and the solution was mixed and incubated for a final 3 min. At the end of the last incubation, 0.5 ml of naphthylethylenediamine solution was added, the mixtures were shaken vigorously, and the absorbances of the samples were read at 530 nm. γ-GT activity was determined from a standard curve and expressed as units per 10^7 cells.

Statistical analysis. All experiments were conducted in triplicate or duplicate wells, with the means from three or four individual experiments used for statistical analysis. The statistical significance of the results was determined by analysis of variance or Student's *t* test. *P* values of < 0.05 were considered statistically significant.

RESULTS

Cell proliferation and virus production by C1-*ts*1-*S* astrocytes. When C1-*ts*1-S cells and C1 cells were cultured side by side for 24, 48, 72, 96, and 120 h, the C1-*ts*1-S cell cultures proliferated more slowly than uninfected C1 cells (Fig. 1A) and contained significantly fewer cells in the S phase at 72 and 120 h (Fig. 1B). When C1-*ts*1-S cells were cultured for 3 or 5 days alongside C1 cells infected with *ts*1 (C1-*ts*1), the acutely infected C1-*ts*1 astrocytes produced more virus at both time points than did the C1-*ts*1-S cells (Fig. 1C). Despite the unique characteristics of C1-*ts*1-S cells, however, their *ts*1 progeny virus retained the specific phenotypic characteristics of the original *ts*1 inoculum. These characteristics included a temperature-sensitive phenotype (41), the ability to infect and kill previously unchallenged astrocyte cultures, and the ability to cause hind-limb paralysis on schedule in neonatally infected FVB/N mice (data not shown).

Upregulation of Bcl-2 and catalase in C1-*ts*1-S cells. Overexpression of the mitochondrial protein Bcl-2 has been shown to block apoptosis in many cell types (14, 29). Work by others has shown that expression of transgenic Bcl-2 in neurons, driven by a neuron-specific promoter, prevents neuronal apoptosis in mice infected with *ts*1 (14). In view of this, we were curious to know how Bcl-2 levels change over time in culture for acutely infected C1-*ts*1 cells relative to C1 cells from 24, 48, or 72 h after infection or for C1-*ts*1-S cells relative to C1 cells after 24, 48, or 72 h of culture. The data in Fig. 2A show that

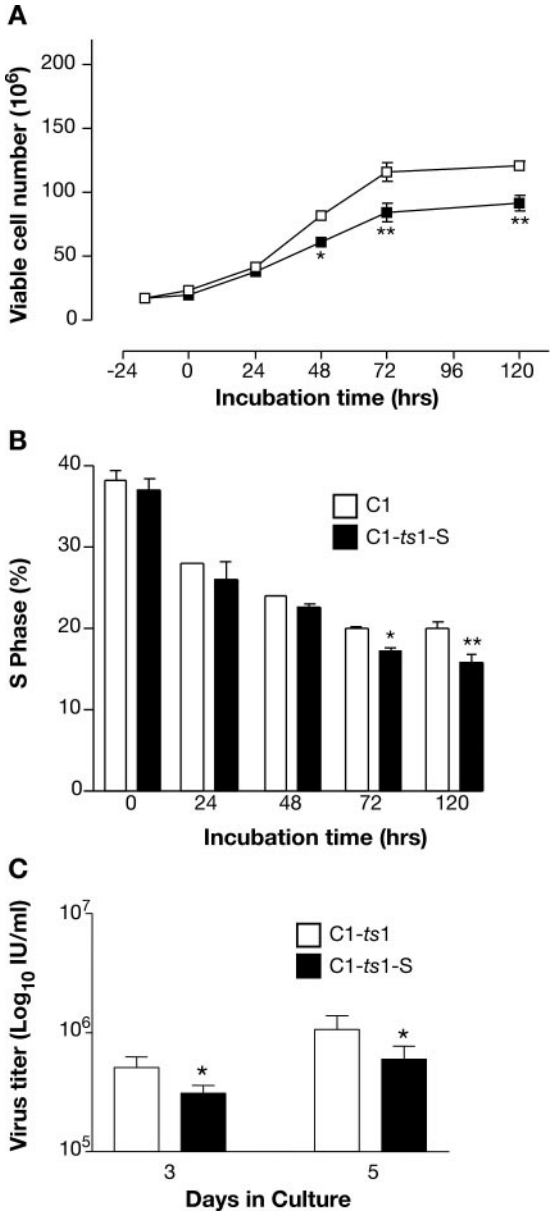

FIG. 1. Characterization of C1-*ts*1-S cells. (A) Cell proliferation rates in C1 and C1-*ts*1-S cell cultures. C1 and C1-*ts*1-S cells were synchronized for 16 h and then incubated for 0, 24, 48, 72, 96, and 120 h. Viable cells were counted daily by trypan blue exclusion. C1 cells (□); C1-*ts*1-S cells (■). ✱, $P < 0.05$; ✱✱, $P < 0.01$ compared with C1 cells. (B) Changes in relative numbers of cells in S phase with time after synchronization in C1 and C1-*ts*1-S cells. C1 and C1-*ts*1-S cells were synchronized for 16 h. After incubation for 0, 24, 48, 72, and 120 h, the cells were fixed in 70% ethanol and stained with propidium iodide containing RNase. The percentages of cells in S phase were determined by fluorescence-activated cell sorter analysis. ✱, $P < 0.05$; ✱✱, $P < 0.01$ compared with C1 cells. (C) Supernatant virus titers from cultures of acutely *ts*1-infected C1 cells (C1-*ts*1) versus C1-*ts*1-S cells, measured at 3 and 5 days p.i. ✱, $P < 0.05$ by *t* test. (A to C) Results shown are the averages from four experiments plus or minus standard deviations.

Bcl-2 levels declined dramatically by 72 hours p.i. in acutely infected (C1-*ts*1) astrocytes relative to uninfected astrocytes. However, Fig. 2B shows that C1-*ts*1-S astrocytes were very different, having significantly higher Bcl-2 levels than uninfected C1 cells at 24, 48, and 72 h of culture. This difference suggests that maintenance of higher than normal Bcl-2 levels may contribute to the survival of C1-*ts*1-S cells after *ts*1 infection.

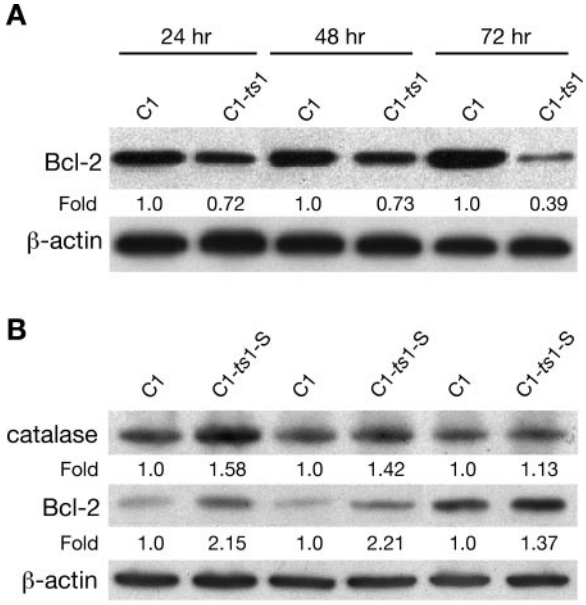

FIG. 2. Bcl-2 in C1 versus C1-*ts*1 cells and in C1 versus C1-*ts*1-S cells. C1, C1-*ts*1, and C1-*ts*1-S cell lysates were prepared after 24, 48, and 72 h of incubation or after infection. Bcl-2 and catalase levels were analyzed by Western blotting. The blots were then stripped and reimmunoblotted with anti-β-actin antibody. (A) Bcl-2 levels in uninfected C1 cells versus C1-*ts*1 cells assayed at 24, 48, and 72 hours p.i. (B) Bcl-2 and catalase levels in uninfected C1 cells versus C1-*ts*1-S cells at 24, 48, and 72 h of culture. The results are representative of three separate experiments. "Fold" values appearing under the bands are ratios of band density, measured by densitometric tracing, to the band density for C1 control cells after normalization for protein loading using the β-actin bands.

We have reported previously that levels of the H_2O_2-scavenging enzyme catalase are reduced after acute infection in C1-*ts*1 cells compared with uninfected C1 cells (20). The Western blotting data in Fig. 2B show that C1-*ts*1-S cells differ from C1-*ts*1 cells in this respect as well, in that catalase protein levels are slightly increased at 24 and 48 hours p.i. in C1-*ts*1-S cells.

Upregulation of ER chaperone proteins. ER chaperone proteins, such as the glucose-responsive proteins 78 and 94 (GRP78 and GRP94) and CalR, are activated by the presence of misfolded proteins in the ER (16). We have shown previously that amounts of GRP78 and GRP94 are elevated in acutely infected C1 astrocytes within 24 hours p.i. (27). In most cell types, ER stress causes Ca^{2+} release from ER stores and is accompanied by rising CalR levels (11). We therefore used Western blotting to compare the levels of these three proteins (GRP78, GRP94, and CalR) over 24, 48, and 72 h of culture for C1-*ts*1-S cells versus uninfected C1 cells. In these experiments, parallel cultures of both cell types were also either left untreated or treated with the GSH synthesis inhibitor BSO.

Figure 3 shows that C1-*ts*1-S cells contained significantly increased levels of GRP78, GRP94, and CalR, relative to uninfected C1 astrocytes, at all three time points. Treatment with BSO increased the expression of ER chaperone proteins in

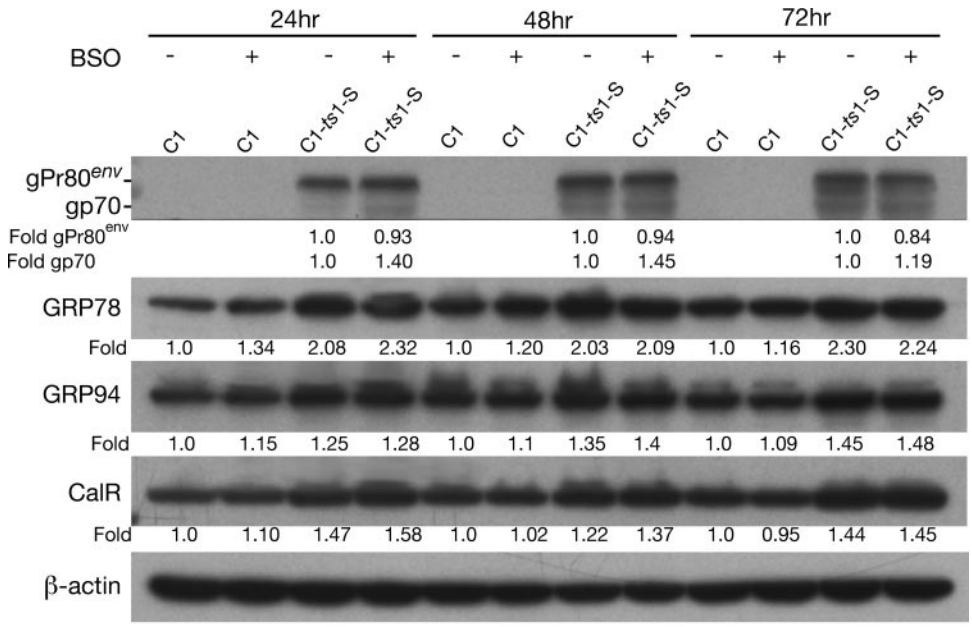

FIG. 3. gPr80^{env} and gp70, GRP78, GRP94, and CalR protein expression in C1 and C1-*ts*1-S cells. C1 or C1-*ts*1-S cells were plated as described in Materials and Methods, but in separate sets of replicate cultures, with one set left untreated and the other treated with 1 mM BSO for the last 24 h of incubation. After incubation for 24, 48, and 72 h, cell lysates were prepared, and 50 μg of total protein from each lysate was analyzed by Western blotting for gPr80^{env} and gp70, GRP78, GRP94, and CalR. The blots were then stripped and reimmunoblotted with anti-β-actin antibody. The results are representative of two or three experiments. The values under the bands are ratios of band density, measured by densitometric tracing, to the band densities for C1 control cells after normalization of protein loading using the β-actin bands.

C1-*ts*1-S cells, but not in C1 cells, at 24 h of culture. This suggested to us that the antioxidant defense machinery represented by these stress proteins is primed and ready for quick response to further challenge (BSO) in C1-*ts*1-S cells.

Lower intracellular ROS levels in C1-*ts*1-S cells. Intracellular H_2O_2 content is a global reflection of amounts of toxic ROS in cells, including H_2O_2, superoxide, and hydroxyl radicals. Using flow cytometry and a fluorescent dye to detect and quantitate intracellular H_2O_2, we have shown previously that acute *ts*1 infection leads to the rapid accumulation of intracellular ROS, and to oxidative stress, in primary astrocyte cultures or in cultured C1 astrocytes (27). The same H_2O_2 measurement protocol was used here to measure ROS levels in (i) C1-*ts*1-S cultures incubated for 24, 48, and 72 h; (ii) acutely infected C1 cell cultures (C1-*ts*1) incubated for 24, 48, and 72 hours p.i.; and (iii) uninfected C1 cell cultures sampled at the same time points. The cells were loaded with CM-H_2DCFDA for 30 min prior to being harvested, as described previously (27), allowing detection of H_2O_2 levels in the cells via the fluorescent derivative formed by interaction of the dye with intracellular H_2O_2.

Figure 4 shows the fluorescence intensity profiles (reflecting H_2O_2 contents) for all three cell types after seeding of cultures (C1-*ts*1-S cells) or after infection (C1 cells) for 24 h (top), 48 h (middle), and 72 h (bottom). The data show that C1-*ts*1-S cells maintained low H_2O_2 (ROS) concentrations, similar to those of uninfected C1 cells, at all three time points, in contrast to high levels at all three time points for acutely infected C1-*ts*1 cells. This difference was particularly evident at 72 h of culture.

Increased intracellular thiols, cystine uptake, and GSH recycling. We have shown previously that thiol-related antioxidative-defense responses are activated after acute infection of C1 astrocytes with *ts*1, but that half of the cells in such cultures still die soon after infection (27). Data from these earlier studies implicated Nrf2 as the factor orchestrating thiol redox responses in infected cells, including increased expression of the xCT cystine/glutamate antiporter, as well as elevations in the levels of specific proteins involved in GSH synthesis. In these prior studies, cells harvested from acutely *ts*1-infected C1-*ts*1 cell cultures (containing both dying cells and the precursors of survivor cells) contained net amounts of GSH significantly lower than those of uninfected C1 cells, although intracellular cysteine levels and consumption of extracellular cystine were both increased (27).

To determine whether the same situation existed in cultures of C1-*ts*1-S cells, we compared the GSH contents of C1-*ts*1-S cells to the GSH contents of uninfected C1 cells, or acutely infected C1-*ts*1 cells, at 24, 48, and 72 hours p.i. Figure 5A shows that the GSH levels of C1-*ts*1-S cells were significantly higher than those of either C1-*ts*1 cells or uninfected C1 cells at 48 to 72 h of culture. This result is very different from that obtained in our earlier work for unseparated *ts*1-infected C1 cell cultures, where net levels of GSH were significantly lower for infected versus uninfected C1 cells (27). Figure 5B shows that intracellular cystine/cysteine levels were also significantly higher in C1-*ts*1-S cultures than in uninfected C1 cultures. We suggest that the maintenance of high levels of GSH in C1-*ts*1-S cells reflects the successful activation of thiol redox defenses in these adapted cells.

In CNS glial cells, including astrocytes, the xCT antiporter at the plasma membrane exchanges incoming cystine for outgoing glutamate. We therefore asked whether the increased

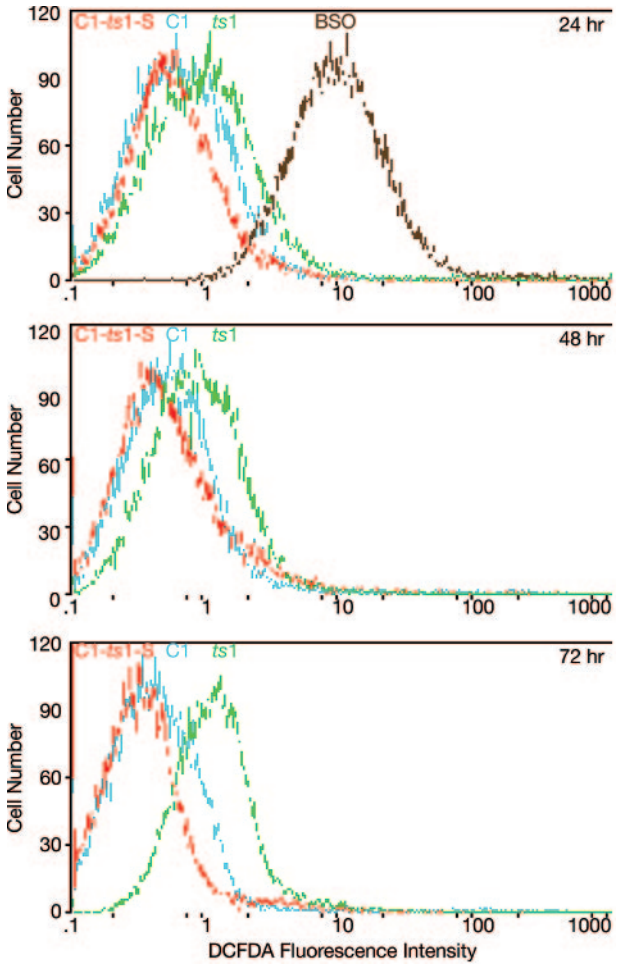

FIG. 4. Intracellular H_2O_2 in C1 and C1-*ts*1-S cells. Intracellular H_2O_2 levels were measured via CM-H_2DCFDA fluorescence in uninfected and acutely infected C1 cells or C1-*ts*1-S cells. After incubation for 24, 48, and 72 h, all cells were loaded with 10 μM CM-H_2DCFDA for 30 min, followed by flow cytometric measurement of their H_2O_2 contents. The three panels represent the results for cells harvested at 24 (top), 48 (middle), and 72 (bottom) hours p.i. Shown are uninfected C1 cells (C1; blue lines), acutely *ts*1-infected C1 cells (*ts*1; green lines), C1-*ts*1-S cells (C1-*ts*1-S; red lines), and BSO-treated C1 cells (BSO; brown lines).

amounts of intracellular GSH and cystine/cysteine in C1-*ts*1-S cells might be due to increased activity of their xCT, which could counteract depletion of GSH in the cells resulting from infection. Figure 5C shows that C1-*ts*1-S cells exhibit significantly increased uptake of [^{35}S]cystine at 24 h of culture compared with uninfected C1 cells. We then also asked whether the increased GSH and cystine/cysteine contents of C1-*ts*1-S cells might be due to enhancement of their GSH salvage pathways via the ectoenzyme γ-GT, which cleaves extracellular GSH into its peptide components, thereby freeing cystine/cysteine for reuptake (8). Figure 5D shows that γ-GT enzymatic activity was increased twofold in C1-*ts*1-S cells at 24 h of culture relative to that measured in uninfected C1 cells. Additional evidence for specific enhancement of γ-GT activity in C1-*ts*1-S cells is provided by the data for C1-*ts*1-S cells and C1 cells treated with the γ-GT-inhibiting agent acivicin, which significantly reduced γ-GT activity in both (Fig. 5D).

Upregulated Nrf2 and its downstream targets. The data above suggested that increased intracellular GSH in C1-*ts*1-S cells is likely to result from upregulation of proteins involved in the Nrf2-mediated thiol antioxidant pathway. As noted above, one of the target genes in this pathway is the xCT antiporter, whose activity is increased in C1-*ts*1-S cells relative to uninfected C1 cells (Fig. 5C). We have shown previously that Nrf2 activation and nuclear translocation, and upregulation of Nrf2 target genes, occur in C1 cells infected with *ts*1 (27).

Activation of the Nrf2 transcription factor begins with its release from its cytoplasmic inhibitor and its translocation into the nucleus (12, 13, 26). In the nucleus, Nrf2 binds to ARE promoter regions in the genes encoding xCT, the two subunits of γ-glutamylcysteine ligase (γ-GCL), γ-GCLC and γ-GCLM, and glutathione peroxidase (GPx) (27).

To test for Nrf2 activation in C1-*ts*1-S cells versus C1 cells, and to determine whether Nrf2 target genes are upregulated in C1-*ts*1-S cells, we cultured C1-*ts*1-S cells and C1 cells side by side for 24, 48, and 72 h. Both cell types were cultured in either the presence or absence of the γ-GCLC inhibitor BSO, which depletes intracellular GSH and activates Nrf2 (27). We sampled the C1-*ts*1-S and C1 cells at each time point, to follow levels of xCT, γ-GCLC, γ-GCLM, and GPx in untreated and BSO-treated C1 versus C1-*ts*1-S cells. Figure 6A shows that nuclear levels of Nrf2 are significantly increased in untreated C1-*ts*1-S cells versus C1 cells at 24, 48, and 72 h of culture and that nuclear Nrf2 levels also rise in the uninfected control C1 cells at 72 h of culture. We suspect that nuclear Nrf2 and Nrf2 target gene expression levels rise at later times in uninfected C1 cells because the cells are growing in spent medium and are becoming oxidatively stressed.

Figure 6B shows that levels of all four of the selected Nrf2 target gene products (xCT, γ-GCLC, γ-GCLM, and GPx) were increased in C1-*ts*1-S cells versus uninfected C1 cells at 24 and 48 h of culture. The transient increase in nuclear translocation of Nrf2 at 24 h of culture in C1-*ts*1-S cells (Fig. 6A), followed by upregulation in levels of its target gene products, most likely reflects the activation sequence itself, in which Nrf2 nuclear translocation, and Nrf2 engagement of ARE sequences in target gene promoters, is followed by transcription and translation of target gene proteins. Treatment of the C1 cells and C1-*ts*1-S cells with the γ-GCLC inhibitor BSO increased Nrf2 expression and Nrf2 target gene expression at all time points for both cell types (Fig. 6A and B).

These results show that Nrf2 activation, Nrf2 nuclear translocation, and specific transcriptional activation of Nrf2 target genes are continuously under way in C1-*ts*1-S cells and that all of these activities are upregulated by BSO.

Cystine/cysteine deficiency increases sensitivity to *ts*1-induced cell death. The availability of cystine/cysteine is a limiting factor for protein and GSH synthesis in both normal and stressed cells (15). For this reason, cystine/cysteine deprivation causes rapid cell death in acutely infected C1 cells (27). We therefore asked whether and how the availability of cystine/cysteine affects intracellular GSH levels and cell survival over time in C1-*ts*1-S cells versus uninfected C1 cells. C1-*ts*1-S cells and C1 cells were cultured for 24, 48, and 72 h in culture medium containing stepped concentrations of cystine (0, 10, 100, 200, and 1,000 μM, where 200 μM is the concentration normally present in C1 cell culture medium). The three graphs on the left of Fig. 7

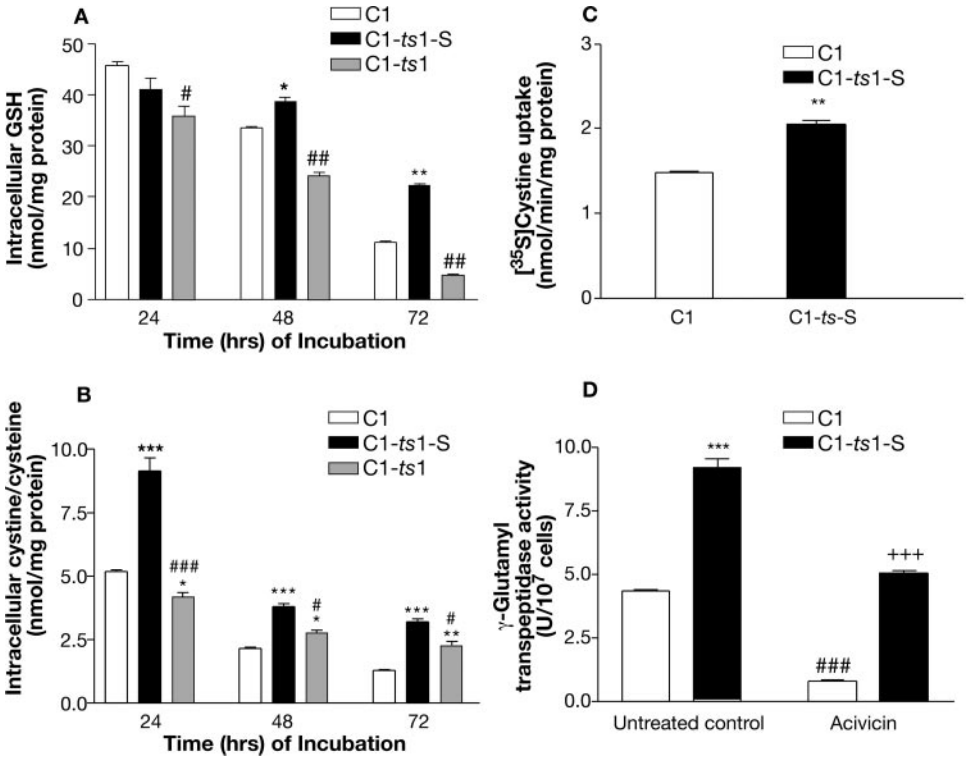

FIG. 5. Intracellular GSH and cystine/cysteine levels, cystine uptake, and γ-GT activities in C1 and C1-*ts*1-S cells. (A) GSH levels in C1 cells, C1-*ts*1-S cells, and acutely infected C1 cells. GSH levels were determined for each culture using a GSH assay kit following the manufacturer's instructions. ⋆, $P < 0.05$; ⋆⋆, $P < 0.01$, comparing C1-*ts*1-S cells with C1 cells. #, $P < 0.05$; ##, $P < 0.01$, for acutely infected C1-*ts*1 cells versus C1-*ts*1-S cells. (B) Intracellular cystine/cysteine levels in C1 and C1-*ts*1-S cells. Total intracellular cysteine was measured by fluorometric HPLC. ⋆, $P < 0.05$; ⋆⋆, $P < 0.01$; ⋆⋆⋆, $P < 0.001$, comparing C1-*ts*1-S and C1-*ts*1 cells with C1 cells at 24, 48, and 72 h, respectively. #, $P < 0.05$; ###, $P < 0.001$, for C1-*ts*1 cells versus C1-*ts*1-S cells. (C) Uptake of [^{35}S]cystine at 24 hours p.i. Cells were incubated in bicarbonate buffer for 20 min prior to the addition of 0.5 μCi/ml of L-[^{35}S]cystine. The cells were then incubated for 3 min, washed, and solubilized for liquid scintillation counting and for protein determination. [^{35}S]cystine uptake rates are shown. ⋆⋆, $P < 0.01$, for C1-*ts*1-S cells versus C1 cells. (D) γ-GT activities in C1 and C1-*ts*1-S cells at 24 hours p.i. C1 or C1-*ts*1-S cells were either left untreated or treated with 200 μM of acivicin for the last 4 h of their 24-hour incubation. γ-GT enzymatic activity in whole-cell lysates was determined using a commercially available γ-glutamyl transferase kit, according to the manufacturer's instructions. γ-GT activity was taken from a standard curve. ⋆⋆⋆, $P < 0.001$, for untreated C1-*ts*1-S cells versus untreated C1 cell controls. ###, $P < 0.001$, for acivicin-treated C1 cells versus untreated C1 cell controls. +++, $P < 0.001$, for acivicin-treated C1-*ts*1-S cells versus untreated C1-*ts*1-S cell controls. All bars reflect means plus or minus standard deviations from two to four independent experiments.

(Fig. 7A, 24, 48, and 72 h) follow viable-cell numbers over time in cultures of C1 versus C1-*ts*1-S cells grown in culture media containing the different cystine concentrations identified above. The three graphs on the right (Fig. 7B) follow intracellular GSH levels under the same conditions.

Figure 7A shows that when numbers of surviving cells at 24, 48, and 72 h for the two cell types are compared, it is clear that C1-*ts*1-S cells die much faster than uninfected C1 cells when cystine is limited or absent. When cultured in 10 μM cystine, for example, C1-*ts*1-S cells survived for 24 h (Fig. 7A, top) but were dead by 48 h (Fig. 7A, middle), although uninfected C1 cells remained alive at all three time points at this cystine concentration (Fig. 7A, top, middle, and bottom). However, at high cystine concentrations (between 100 and 1,000 μM), viable-cell counts for C1-*ts*1-S cells were actually higher than those of uninfected C1 cells, even at 72 h of culture. It appears that although C1-*ts*1-S cells are more sensitive to cystine/cysteine deficiency than are uninfected C1 cells; they use cystine more efficiently than do uninfected C1 cells at higher cystine concentrations.

The three graphs in Fig. 7B follow intracellular GSH levels over time (24, 48, and 72 h) in C1 versus C1-*ts*1-S cells, again cultured in stepped concentrations of cystine. As expected from the data in Fig. 7A, intracellular GSH levels in C1-*ts*1-S cells at 48 and 72 h of culture were significantly higher than those of C1 cells at cystine concentrations close to those in normal cell culture medium (compare the two bottom graphs in Fig. 7B to the top graph), and C1-*ts*1-S cells maintained constant GSH levels over the entire experimental period when cultured at the highest cystine concentration (1,000 μM), while GSH levels in C1 cells declined over time.

Together, these observations show that C1-*ts*1-S cells are less able than C1 cells to survive cystine-limiting culture conditions and to maintain intracellular GSH homeostasis at low cystine concentrations (<10 μM) (Fig. 7A, 48 and 72 h of culture). On the other hand, C1-*ts*1-S cells use cystine more efficiently than C1 cells, both for survival and for GSH synthesis, when cultured at normal or higher than normal cystine concentrations (100, 200, and 1,000 μM cystine) (Fig. 7A and B).

GSH and cystine/cysteine levels in the *ts*1-infected brainstem and spinal cord. Work by others has shown that whole CNS tissues and cerebrospinal fluid of HIV-infected patients

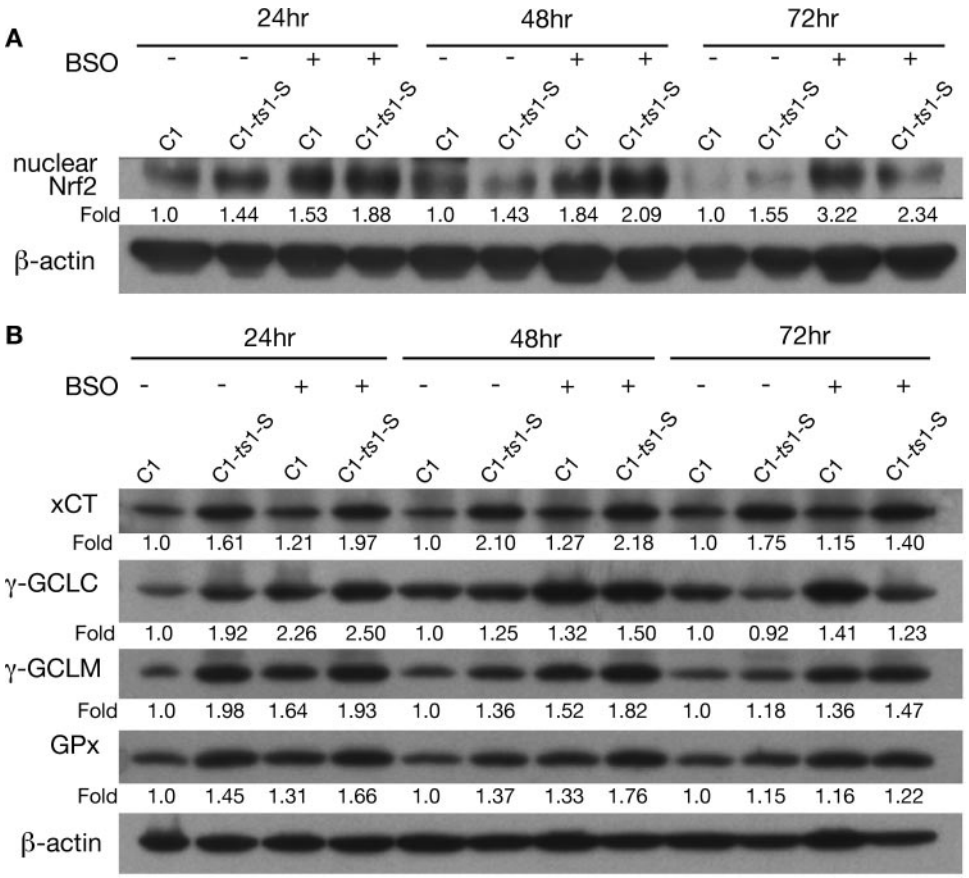

FIG. 6. Transient upregulation of Nrf2 and activation of its downstream target genes xCT, γ-GCL subunits, and GPx in C1-*ts*1-S cells. (A) C1 or C1-*ts*1-S cells were incubated for 24, 48, and 72 h in the presence or absence of BSO for the last 24 h of their incubation. For cells harvested at each time point, nuclear lysates were prepared and analyzed for their content of Nrf2. (B) C1 or C1-*ts*1-S cells were incubated for 24, 48, and 72 h in the presence or absence of BSO for the last 24 h of their incubation. For cells harvested at each time point, nuclear lysates were prepared and analyzed for their content of xCT, γ-GCLC and γ-GCLM, and GPx. All blots were stripped and reimmunoblotted with anti-β-actin antibody as a protein loading control. All blots shown are representative of three or four independent experiments. The values under the bands are ratios of band density, measured by densitometric tracing, to the band densities of C1 control cells after normalization of protein loading using the β-actin bands.

contain decreased levels of GSH relative to those of uninfected individuals (25). In spongiform lesions of the brainstems and spinal cords of *ts*1-infected mice, we found larger numbers of cells containing malondialdehyde adducts, which are protein-malondialdehyde complexes produced by membrane lipid peroxidation, reflecting oxidative stress (13a). We therefore compared cystine/cysteine and GSH in whole brainstem tissues of *ts*1-infected versus uninfected mice at 30 days p.i. to assess the relationship between precursor and product (cystine/cysteine and GSH) in whole CNS tissue from infected mice. Figures 8A and B show that cystine/cysteine levels, but not GSH levels, were reduced in the infected CNS tissues compared to control CNS tissues at 30 days p.i. These observations suggest that thiol-related antioxidant responses are activated in the *ts*1-infected CNS at this time point (high GSH levels in the tissues) but that substrate depletion is also under way (lower cystine/cysteine levels).

DISCUSSION

The genetic determinant of neurovirulence in *ts*1 is a single-point mutation in its *env* sequence, which results in a Val-25→Ile substitution in the precursor envelope protein gPr80^{env} (39). Due to this substitution, the *ts*1 gPr80^{env} precursor protein accumulates in the ER of cultured astrocytes (33, 39, 47), inducing ER stress. ER stress responses lead to increased intracellular production of GADD153, release of Ca^{2+} from ER stores, and mitochondrial stress (19). These events are associated with ROS accumulation (27).

Our published studies have shown that cultured astrocytes respond to *ts*1 infection, and to the events described above, by activation of specific thiol antioxidant defenses linked to the activation of Nrf2 (18, 19, 27, 33, 37). In this study, we asked which of these defenses are activated in the "survivor" cell population that arises in long-term *ts*1-infected astrocyte cultures. We therefore established a population of "survivor" *ts*1-infected C1 cells (C1-*ts*1-S) from the C1 astrocytic cell line and compared cell growth, virus production, and thiol- and non-thiol-related antioxidant defenses in these cells to those of uninfected C1 cells or acutely infected C1 cells. We first observed that C1-*ts*1-S cells exhibited slower growth than uninfected C1 cells and that they maintained lower levels of viral replication relative to acutely infected C1 cells. It seemed likely that slowed cell proliferation and restricted virus production in

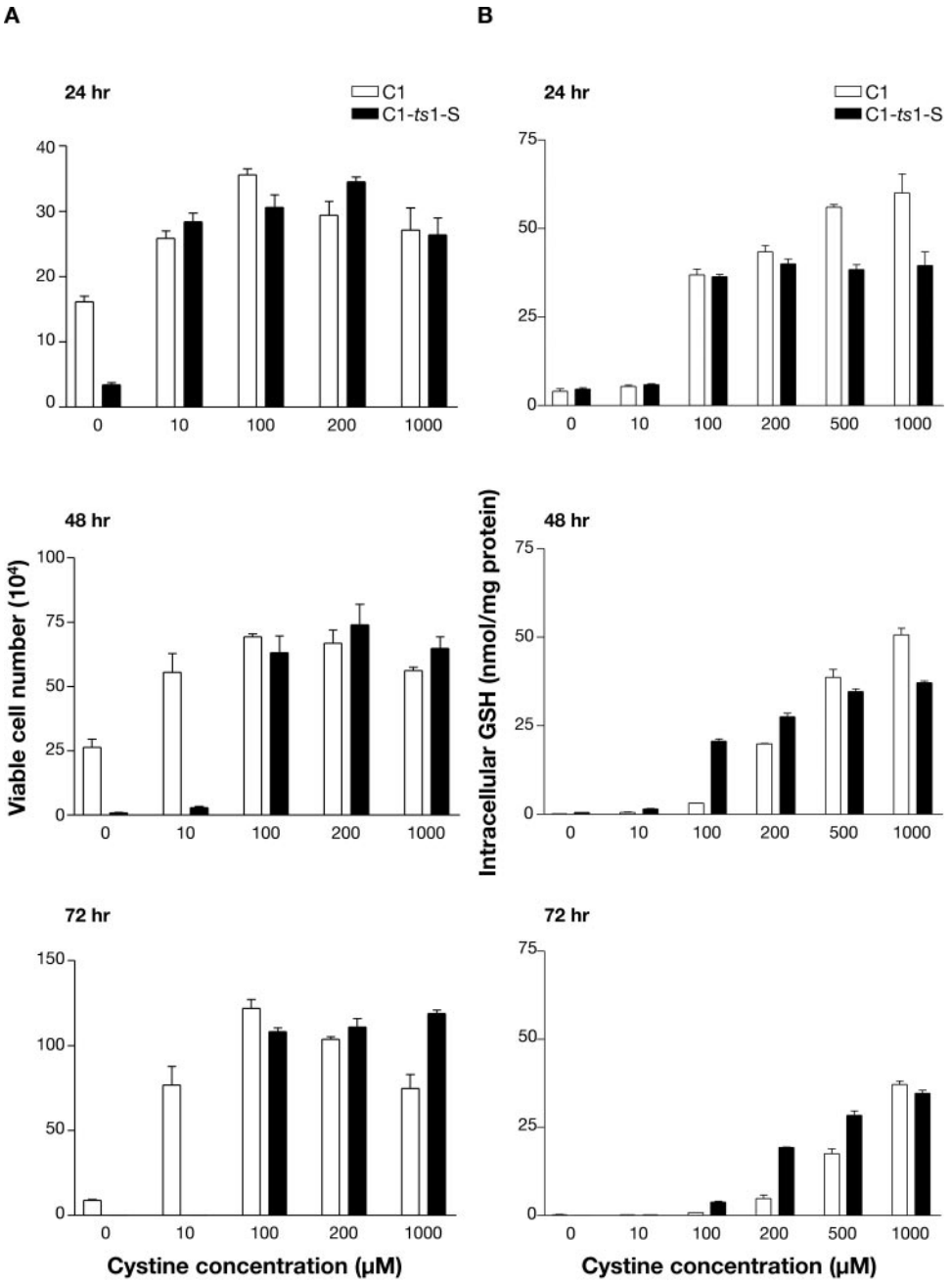

FIG. 7. Cell numbers and GSH levels at 24, 48, and 72 h of culture in C1 and C1-*ts*1-S cells grown in cystine-deficient medium. C1 or C1-*ts*1-S cells were plated in 60-mm dishes and cultured in cystine-free DMEM with 10% FBS, supplemented with the indicated concentrations of cystine, and incubated for 24, 48, and 72 h. (A) Cell viability assays at 24 (top), 48 (middle), and 72 (bottom) hours p.i. Viable cells were counted by trypan blue exclusion. The results are the means plus standard deviations for three different experiments. (B) Intracellular GSH levels, measured as described in Materials and Methods, for cells grown as described for panel A, for 24 (top), 48 (middle), and 72 (bottom) hours p.i. The results are the means plus standard deviations for three different experiments.

C1-*ts*1-S cells occur because some cell resources are diverted to mechanisms for virus production, thereby reducing the supply of energy available for normal cellular protein synthesis and proliferation. Among these cellular resources, we suspected that cystine/cysteine supplies in particular are likely to be redirected for use in antioxidant defenses against viral infection, detracting from their availability for cell proliferation and protein synthesis. We therefore tested this hypothesis, and we report here that the successful deployment of these particular defenses, i.e., thiol antioxidant pathways, is central to the survival of astrocytes after *ts*1 infection.

Nrf2 activation mobilizes thiol oxidant defenses by upregulating transcription of genes involved in the biosynthesis of GSH. The proteins encoded by these genes include the plasma membrane xCT antiporter, the catalytic and modulatory subunits of γ-GCL, and GPx (21). Cystine is reduced to cysteine

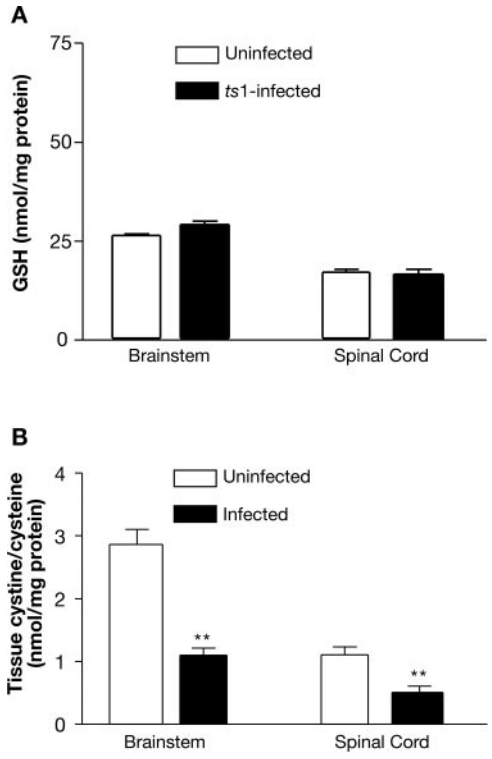

FIG. 8. Total brainstem and spinal cord GSH and cystine/cysteine at 30 days p.i. (A) GSH levels in brainstem and spinal cord tissues from uninfected versus *ts*1-infected mice at 30 days p.i. (B) Cystine/cysteine levels in brainstem and spinal cord tissues of uninfected and *ts*1-infected mice at 30 days p.i. The data are expressed as the means plus or minus standard deviations for five to eight mice for each determination. In panel B, **, $P < 0.01$ for *ts*1-infected versus uninfected mice.

upon entry into the cell, and this cysteine provides the substrate for the heterodimeric enzyme γ-GCL, which catalyzes the rate-limiting step in the synthesis of γ-glutamylcysteine, a precursor of GSH (5, 34). GSH protects oxidatively stressed cells by reacting directly with oxygen or nitrogen free radicals and by donating electrons for reduction of H_2O_2 to H_2O by GPx (6, 7, 23, 25, 32).

C1-*ts*1-S astrocytes tolerate viral infection by mobilizing Nrf2-mediated thiol antioxidant defenses, with upregulation of xCT, cystine uptake, and GSH synthesis. Both subunits of γ-GCL (γ-GCLC and γ-GCLM) are upregulated, as are GPx levels. As expected under these conditions, intracellular GSH levels in C1-*ts*1-S cells are significantly increased relative to those of uninfected or acutely infected C1 cells, but this occurs only if sufficient cystine is available in the culture medium. Cystine uptake is the rate-limiting step for GSH production, and large amounts of cystine must be available in the medium if demand for GSH is increased. As expected, therefore, C1-*ts*1-S cells maintain normal ROS levels and GSH content when the culture medium contains nonlimiting concentrations of cystine but quickly die at low concentrations of cystine.

It is significant that the result of this pattern of adaptations in C1-*ts*1-S cells (maintenance of protective levels of intracellular GSH) is quite distinct from events that occur in unseparated *ts*1-infected C1 cells, which also activate Nrf2-mediated defenses but half of which die (27). C1-*ts*1-S cells can maintain high cystine/cysteine and GSH levels, and low intracellular ROS, over 72 h of culture while they survive, divide, and produce virus. By contrast, cystine/cysteine and GSH levels of C1-*ts*1 cells begin to decline at early times after infection, and their intracellular ROS levels rise and remain high until the cells die (by 72 hours p.i.). At present, we do not know why these two distinct cell types arise in synchronized C1 cell cultures whose infection conditions should ensure simultaneous infection of all cells. We suspect that the answer to this question may provide valuable information about conditions that suppress or promote retroviral infection in CNS tissues. It is interesting to note from this study that cystine/cysteine levels, but not GSH levels, were reduced in whole infected CNS tissues, compared to control CNS tissues, at 30 days p.i. These observations suggest that thiol-related antioxidant responses are activated in *ts*1-infected CNS tissues at this time point (high GSH levels in the tissues) but that substrate depletion is also under way (lower cystine/cysteine levels). Work is now in progress in our laboratory to measure these parameters for individual cell types in the CNS.

C1-*ts*1-S cells also mobilize other antiapoptotic and antioxidant defenses, including catalase, the antiapoptotic Bcl-2 protein, and ER chaperones. The mechanism for upregulation of these proteins is unclear. We postulate that since all of these proteins are redox sensitive, their increased levels could be a response to infection-induced changes in the intracellular redox potential (i.e., relative concentrations of oxidants to antioxidants). We are currently carrying out further studies to address these questions.

These results corroborate our earlier (19, 27) and current (13a) findings and support the hypothesis that thiol depletion and oxidative stress are key factors in the pathogenesis of *ts*1-induced neurodegenerative disease. They also suggest that restoration of the cellular redox balance, and of ER homeostasis, may enable some *ts*1-infected astrocytes to survive in vivo and continue to produce low levels of virus. If so, targeted therapies to protect cells against oxidative stress and to restore thiol depletion might be suitable for treatment of this and other retrovirus-induced neurodegenerative diseases (13a).

However, the specific roles played in vivo by possible "survivor" astrocytes in *ts*1-induced neurodegeneration remain unclear. We do know that infected astrocytes are oxidatively stressed and that their ability to supply local neurons with adequate reduced thiols is likely to be compromised whether or not the astrocytes survive infection, and that this may contribute to the death of neurons that are not infected with *ts*1. Interestingly, it has been reported that in HIV type 1 infection of the brain, astrocytes undergo restricted virus replication (28) and survive HIV Tat protein expression by increasing their antioxidant defenses (3). If C1-*ts*1-S cells represent "survivor" astrocytes that arise in the intact CNS of *ts*1-infected mice, such cells may act as persistent viral reservoirs in this and other retroviral infections, including that caused by HIV type 1 (2). If this proves to be the case, the existence of such cells must be taken into account when devising or administering therapies for neurodegeneration following retroviral infection (22, 30). This is because such treatments could activate and promote the proliferation of these cells, thereby facilitating existing productive infection or allowing the reemergence of virus infection and spread in the CNS.

ACKNOWLEDGMENTS

We thank Shawna Johnson, Cynthia Kim, Lisa Whitson, Christine K. Brown, and Joi Holcomb for their excellent assistance in preparing the manuscript. Kent Claypool provided assistance with flow cytometry analysis, and Guoyao Wu (Texas A&M University) provided HPLC expertise. We also thank Terrance Kavanagh (University of Washington, Seattle) for the generous gift of anti-γ-GCLC antibody and Marie H. Hanigan (University of Oklahoma Health Sciences Center, Oklahoma City) for her γ-GT expertise and advice. We are grateful for valuable suggestions provided by Mingshan Yan and Jianjun Shen.

This work was supported by NIH grants NS043954 and MH071583 (to P.K.Y. Wong) and NIEHS Center Grant ES07784 and Core Grant CA16672.

REFERENCES

1. **Bender, A. S., W. Reichelt, and M. D. Norenberg.** 2000. Characterization of cystine uptake in cultured astrocytes. Neurochem Int. **37:**269–276.
2. **Brack-Werner, R.** 1999. Astrocytes: HIV cellular reservoirs and important participants in neuropathogenesis. AIDS **13:**1–22.
3. **Chauhan, A., J. Turchan, C. Pocernich, A. Bruce-Keller, S. Roth, D. A. Butterfield, E. O. Major, and A. Nath.** 2003. Intracellular human immunodeficiency virus Tat expression in astrocytes promotes astrocyte survival but induces potent neurotoxicity at distant sites via axonal transport. J. Biol. Chem. **278:**13512–13519.
4. **Choe, W., G. Stoica, W. Lynn, and P. K. Y. Wong.** 1998. Neurodegeneration induced by MoMuLV-ts1 and increased expression of Fas and TNF-alpha in the central nervous system. Brain Res. **779:**1–8.
5. **Dalton, T. P., M. Z. Dieter, Y. Yang, H. G. Shertzer, and D. W. Nebert.** 2000. Knockout of the mouse glutamate cysteine ligase catalytic subunit (Gclc) gene: embryonic lethal when homozygous, and proposed model for moderate glutathione deficiency when heterozygous. Biochem. Biophys. Res. Commun. **279:**324–329.
6. **Dringen, R.** 2000. Metabolism and functions of glutathione in brain. Prog. Neurobiol. **62:**649–671.
7. **Dringen, R., and B. Hamprecht.** 1997. Involvement of glutathione peroxidase and catalase in the disposal of exogenous hydrogen peroxide by cultured astroglial cells. Brain Res. **759:**67–75.
8. **Dringen, R., B. Hamprecht, and S. Broer.** 1998. The peptide transporter PepT2 mediates the uptake of the glutathione precursor CysGly in astroglia-rich primary cultures. J. Neurochem. **71:**388–393.
9. **Dringen, R., O. Kranich, and B. Hamprecht.** 1997. The gamma-glutamyl transpeptidase inhibitor acivicin preserves glutathione released by astroglial cells in culture. Neurochem. Res. **22:**727–733.
10. **Gonzalez-Scarano, F., N. Nathanson, and P. K. Y. Wong.** 1995. Retroviruses and the nervous system, p. 409–490. *In* J. Levy (ed.), The Retroviridae, vol. 4. Plenum Press, New York, N.Y.
11. **Groenendyk, J., J. Lynch, and M. Michalak.** 2004. Calreticulin, $Ca2^{+}$, and calcineurin—signaling from the endoplasmic reticulum. Mol. Cell **17:**383–389.
12. **Itoh, K., N. Wakabayashi, Y. Katoh, T. Ishii, K. Igarashi, J. D. Engel, and M. Yamamoto.** 1999. Keap1 represses nuclear activation of antioxidant responsive elements by Nrf2 through binding to the amino-terminal Neh2 domain. Genes Dev. **13:**76–86.
13. **Jaiswal, A. K.** 2000. Regulation of genes encoding NAD(P)H:quinone oxidoreductases. Free Radic. Biol. Med. **29:**254–262.
13a. **Jiang, Y., V. L. Scofield, M. Yan, W. Qiang, N. Liu, A. J. Reid, W. S. Lynn, and P. K. Y. Wong.** J. Virol., in press.
14. **Jolicoeur, P., C. Hu, T. W. Mak, J. C. Martinou, and D. G. Kay.** 2003. Protection against murine leukemia virus-induced spongiform myloencephalopathy in mice overexpressing Bcl-2 but not in mice deficient for interleukin-6, inducible nitric oxide synthetase, ICE, Fas, Fas ligand, or TNF-R1 genes. J. Virol. **77:**13161–13170.
15. **Jones, D. P., Y. M. Go, C. L. Anderson, T. R. Ziegler, J. M. Kinkade, Jr., and W. G. Kirlin.** 2004. Cysteine/cystine couple is a newly recognized node in the circuitry for biologic redox signaling and control. FASEB J. **18:**1246–1248.
16. **Kozutsumi, Y., M. Segal, K. Normington, M. J. Gething, and J. Sambrook.** 1988. The presence of malfolded proteins in the endoplasmic reticulum signals the induction of glucose-regulated proteins. Nature **332:**462–464.
17. **LeBel, C. P., S. F. Ali, M. McKee, and S. C. Bondy.** 1990. Organometal-induced increases in oxygen reactive species: the potential of 2′,7′-dichlorofluorescin diacetate as an index of neurotoxic damage. Toxicol. Appl. Pharmacol. **104:**17–24.
18. **Lin, Y. C., C. W. Chow, P. H. Yuen, and P. K. Y. Wong.** 1997. Establishment and characterization of conditionally immortalized astrocytes to study their interaction with ts1, a neuropathogenic mutant of Moloney murine leukemia virus. J. Neurovirol. **3:**28–37.
19. **Liu, N., X. Kuang, H. T. Kim, G. Stoica, W. Qiang, V. L. Scofield, and P. K. Y. Wong.** 2004. Possible involvement of both endoplasmic reticulum- and mitochondria-dependent pathways in MoMuLV-ts1-induced apoptosis in astrocytes. J. Neurovirol. **10:**189–198.
20. **Liu, N., W. Qiang, X. Kuang, P. Thuillier, W. S. Lynn, and P. K. Y. Wong.** 2002. The peroxisome proliferator phenylbutyric acid (PBA) protects astrocytes from ts1 MoMuLV-induced oxidative cell death. J. Neurovirol. **8:**318–325.
21. **Lu, S. C.** 1998. Regulation of hepatic glutathione synthesis. Semin. Liver Dis. **18:**331–343.
22. **Lynn, W. S., and P. K. Y. Wong.** 1995. Neuroimmunodegeneration: do neurons and T cells use common pathways for cell death? FASEB J. **9:**1147–1156.
23. **McClung, C. R.** 1997. Regulation of catalases in Arabidopsis. Free Radic. Biol. Med. **23:**489–496.
24. **Misra, I., and O. W. Griffith.** 1998. Expression and purification of human gamma-glutamylcysteine synthetase. Protein Expr. Purif. **13:**268–276.
25. **Mollace, V., H. S. Nottet, P. Clayette, M. C. Turco, C. Muscoli, D. Salvemini, and C. F. Perno.** 2001. Oxidative stress and neuroAIDS: triggers, modulators and novel antioxidants. Trends Neurosci. **24:**411–416.
26. **Prestera, T., and P. Talalay.** 1995. Electrophile and antioxidant regulation of enzymes that detoxify carcinogens. Proc. Natl. Acad. Sci. USA **92:**8965–8969.
27. **Qiang, W., J. M. Cahill, J. Liu, X. Kuang, N. Liu, V. L. Scofield, J. R. Voorhees, A. J. Reid, M. Yan, W. S. Lynn, and P. K. Y. Wong.** 2004. Activation of transcription factor Nrf-2 and its downstream targets in response to Moloney murine leukemia virus *ts*1-induced thiol depletion and oxidative stress in astrocytes. J. Virol. **78:**11926–11938.
28. **Ranki, A., M. Nyberg, V. Ovod, M. Haltia, I. Elovaara, R. Raininko, H. Haapasalo, and K. Krohn.** 1995. Abundant expression of HIV Nef and Rev proteins in brain astrocytes in vivo is associated with dementia. AIDS **9:**1001–1008.
29. **Reed, J. C.** 1994. Bcl-2 and the regulation of programmed cell death. J. Cell Biol. **124:**1–6.
30. **Roederer, M., S. W. Ela, F. J. Staal, and L. A. Herzenberg.** 1992. *N*-Acetylcysteine: a new approach to anti-HIV therapy. AIDS Res. Hum. Retrovir. **8:**209–217.
31. **Saha, K., P. H. Yuen, and P. K. Y. Wong.** 1994. Murine retrovirus-induced depletion of T cells is mediated through activation-induced death by apoptosis. J. Virol. **68:**2735–2740.
32. **Shih, A. Y., D. A. Johnson, G. Wong, A. D. Kraft, L. Jiang, H. Erb, J. A. Johnson, and T. H. Murphy.** 2003. Coordinate regulation of glutathione biosynthesis and release by Nrf2-expressing glia potently protects neurons from oxidative stress. J. Neurosci. **23:**3394–3406.
33. **Shikova, E., Y. C. Lin, K. Saha, B. R. Brooks, and P. K. Y. Wong.** 1993. Correlation of specific virus-astrocyte interactions and cytopathic effects induced by *ts*1, a neurovirulent mutant of Moloney murine leukemia virus. J. Virol. **67:**1137–1147.
34. **Solis, W. A., T. P. Dalton, M. Z. Dieter, S. Freshwater, J. M. Harrer, L. He, H. G. Shertzer, and D. W. Nebert.** 2002. Glutamate-cysteine ligase modifier subunit: mouse Gclm gene structure and regulation by agents that cause oxidative stress. Biochem. Pharmacol. **63:**1739–1754.
35. **Stoica, G., R. Barker, G. Wu, W. S. Lynn, and P. K. Y. Wong.** 1998. Quantitative variation of free amino acids in the central nervous system of MoMuLV-ts1-infected mice. In Vivo **12:**395–401.
36. **Stoica, G., E. Floyd, O. Illanes, and P. K. Y. Wong.** 1992. Temporal lymphoreticular changes caused by ts1, a paralytogenic mutant of Moloney murine leukemia virus TB. Lab. Investig. **66:**427–436.
37. **Stoica, G., O. Illanes, S. I. Tasca, and P. K. Y. Wong.** 1993. Temporal central and peripheral nervous system changes induced by a paralytogenic mutant of Moloney murine leukemia virus TB. Lab. Investig. **69:**724–735.
38. **Stoica, G., S. I. Tasca, and P. K. Y. Wong.** 2000. Motor neuronal loss and neurofilament-ubiquitin alteration in MoMuLV-ts1 encephalopathy. Acta Neuropathol. **99:**238–244.
39. **Szurek, P. F., P. H. Yuen, J. K. Ball, and P. K. Y. Wong.** 1990. A Val-25-to-Ile substitution in the envelope precursor polyprotein, gPr80env is responsible for the temperature sensitivity, inefficient processing of gPr80env, and neurovirulence of ts1, a mutant of Moloney murine leukemia virus TB. J. Virol. **64:**467–475.
40. **Wong, P. K. Y., G. Prasad, J. Hansen, and P. H. Yuen.** 1989. ts1, a mutant of Moloney murine leukemia virus-TB, causes both immunodeficiency and neurologic disorders in BALB/c mice. Virology **170:**450–459.
41. **Wong, P. K. Y., L. J. Russ, and J. A. McCarter.** 1973. Rapid, selective procedure for isolation of spontaneous temperature-sensitive mutants of Moloney leukemia virus. Virology **51:**424–431.
42. **Wong, P. K. Y.** 1990. Moloney murine leukemia virus temperature-sensitive mutants: a model for retrovirus-induced neurologic disorders. Curr. Top. Microbiol. Immunol. **160:**29–60.
43. **Wong, P. K. Y., W. S. Lynn, Y. C. Lin, W. Choe, and P. H. Yuen.** 1998. *ts*1 MoMuLV: a murine model of neuroimmunodegeneration, p. 75–93. *In* P. K. Y. Wong and W. S. Lynn (ed.), Neuroimmunodegeneration. R. G. Landes, Austin, Tex.

44. **Wong, P. K. Y., and P. H. Yuen.** 1992. Molecular basis of neurologic disorders induced by a mutant, *ts*1, of Moloney murine leukemia virus, p. 161–197. *In* R. P. Roos (ed.), Molecular neurovirology: pathogenesis of viral CNS infection. Humana Press, Totowa, N.J.
45. **Wu, G., P. K. Davis, N. E. Flynn, D. A. Knabe, and J. T. Davidson.** 1997. Endogenous synthesis of arginine plays an important role in maintaining arginine homeostasis in postweaning growing pigs. J. Nutr. **127:**2342–2349.
46. **Yu, Y., C. A. Kamps, P. H. Yuen, and P. K. Y. Wong.** 1991. Construction and characterization of expression systems for the *env* gene of *ts*1, a mutant of Moloney murine leukemia virus-TB. Virus Res. **19:**83–92.
47. **Yu, Y., and P. K. Y. Wong.** 1992. Studies on compartmentation and turnover of murine retrovirus envelope proteins. Virology **188:**477–485.
48. **Yuen, P. H., M. M. Soong, M. S. Kissil, and P. K. K. Wong.** 1984. Restriction of Moloney murine leukemia virus replication in Moloney murine sarcoma virus-infected cells. Virology **132:**377–389.